JOURNAL OF MATERIALS SCIENCE **38** (2003) 3325–3330

The effect of preparation method and Sb content on SnO_2-CuO sintering

I. O. MAZALI*, W. C. LAS‡, M. CILENSE
Departamento de Físico-Química, Instituto de Química—UNESP, C.P. 355, Araraquara, SP, Brazil 14801-970
E-mail: wlas@iq.unesp.br

The sintering behavior of SnO_2-CuO system has been investigated for two preparation methods and as a function of antimony concentration. A chemical preparation (Pechini's method) resulted in powders with smaller particle sizes than for a conventional oxide mixture. This led to smaller grain sizes in Pechini's method ceramics. The microstructures were heterogeneous in both systems, showing grain coarsening. The densification was aided by liquid phase formation, due to copper, in both systems, but the temperature of maximum shrinkage rate was larger for the Pechini's method ceramic because copper had to diffuse to the grain surface. Independently of the preparation method, antimony did not aid densification, and increasing its concentration led to a higher densification temperature and lower shrinkage rate.

1. Introduction

Tin dioxide has many applications in industry. It is used as gas sensor [1, 2] and studied as a varistor device material [3, 4]. In the latter case, dense ceramics are required. This is achieved by doping tin dioxide with cations, such as manganese [5, 6], cobalt [7], zinc [8] and copper [6, 9–12]. These cations may favor densification by point defect formation, due to dopant solid solution. Representing transition metal oxides by MO, oxygen vacancy formation can be expressed by:

$$\mathrm{MO} \xrightarrow{\mathrm{SnO_2}} \mathrm{M''_{Sn}} + \mathrm{O_O^x} + \mathrm{V_{\ddot{O}}} \qquad (1)$$

The studies of CuO in tin dioxide densification lead to a general consensus that liquid phase formation is the main densification mechanism at temperatures $\geq$940°C, as reported by the authors mentioned above, except Lalande *et al.* [11] who saw no evidence of liquid formation at $T < 1000$°C. The liquid phase favors grain rearrangement and ensures matter transfer; it controls the densification process with a dissolution-limiting step, between 940 and 1000°C, and with a diffusion-limiting step at higher temperature [9]. Low solubility of SnO_2 in the Cu-rich interstitial phase is reported [10], which is in agreement with the presence of an interganular phase [9, 11] rich in Cu, probably a mixture of CuO and Cu_2O phases, and observed even at low Cu concentration (0.75 wt% $\approx$ 1.4 mol%) [11]. This intergranular phase is reduced or disappears after long-duration heat treatments [9,11]. Below 940°C, however, liquid phase sintering is not seen [11, 12]. Distribution of Cu ions is reported to occur through surface diffusion at temperatures as low as 400°C [12]. Also, oxygen vacancies, which are not free, are located within a thick layer on the grain surface contributing to a viscous-flow sintering mechanism [12]. The increase in oxygen vacancy concentration is shown in Equation 1, with M = Cu.

Dopant segregation seems to be a common phenomenon in SnO_2, as just described for Cu and also for Mn [5, 13] and Sb [14–18].

Antimony oxide is largely utilized to promote the electrical conductivity of tin dioxide based ceramics. However, it is well known in the literature [10, 19, 20] for not densifying tin dioxide, unless by hot isostatic pressing (known as HIP) [20]. It is reported [10] that the decrease in oxygen vacancy concentration, due to its reaction with antimony oxide,

$$\mathrm{Sb_2O_5} + \mathrm{V_{\ddot{O}}} \xrightarrow{\mathrm{SnO_2}} 2\mathrm{Sb''_{Sn}} + 2\mathrm{e^-} + 5\mathrm{O_O^x} \qquad (2)$$

restrains tin dioxide densification.

The objective of the present work was to prepare $Sn_{(0.99-x)}Cu_{0.01}Sb_xO_2$ ceramics, with $0 \leq x \leq 0.01$, by conventional oxide mixture and chemical preparation (Pechini's method, described in Section 2), and to verify the influence of the preparation method and Sb concentration on the sintering behavior of the SnO_2-CuO system. The majority of reports in the literature utilize the conventional oxide mixture and there are almost no citations establishing a comparison between equal composition systems prepared by two different methods.

Temporary address: Laboratório de Química do Estado Sólido, Instituto de Química—UNICAMP, CP 6154, 13083-970 Campinas—SP, Brazil.
‡Author to whom all correspondence should be addressed.

2. Experimental procedure

The conventional oxide mixture was prepared from nominally pure SnO_2, CuO and Sb_2O_3. Powders were mixed in a ball mill for 8 h, in isopropylic alcohol which was eliminated at 120°C for 2 h; next, powders were calcined at 400°C for 2 h.

Chemical powder synthesis was carried out by employing Pechini's method, which makes use of the capability that certain α-hydroxycarboxylic organic acids possess of forming polybasic acid chelates with several cations. When mixing with a polyhydroxylic alcohol and heating, the chelate transforms into a polymer, maintaining the cations in a homogeneous distribution. The organic part is eliminated at low temperatures (≈300°C), forming reactive oxides with well-controlled stoichiometry [21]; more details are given elsewhere [22]. In our case, the material was heat treated at 400°C for 4 h plus 500°C for 15 h. The powders were ball milled and calcined exactly as in the conventional oxide mixture. Cation sources were the following salts, all of analytical grade: $SnCl_2{\cdot}2H_2O$, $Cu(CH_3COO)_2{\cdot}H_2O$ and $H_2[(C_4H_2O_6)_2Sb_2]$; the antimony tartrate synthesis is described elsewhere [23].

Ceramics were prepared in the following compositions: $Sn_{0.99-x}Cu_{0.01}Sb_xO_2$, with $x = 0$, 0.005 and 0.010, for both methods, Pechini and mixture of oxides, abbreviated as Pch and Mox, respectively.

Powder X-ray diffraction (XRD) analysis was performed in a Siemens diffractometer with Cu K_α radiation ($\lambda = 1.5406$ Å) and Ni filter.

Specific surface areas, S_{BET}, were determined from adsorption-desorption experiments, with a nitrogen-helium gas mixture, using the BET method [24]. The mean particle size, D_{BET}, was calculated by:

$$D_{BET} = \frac{6}{(d_{th} \cdot S_{BET})} \tag{3}$$

where d_{th} is the theoretical density in g cm^{-3}; S_{BET} and D_{BET} are given in m^2 g^{-1} and μm, respectively.

The analysis of particle size distribution, S_{SED}, was performed by powder sedimentation measurements carried out in a Sedigraph 5000 ET particle size analyzer, using hexametaphosphate aqueous solution as dispersant in the ultrasound bath. S_{SED} values were taken at 50% of accumulative mass.

Powders were uniaxially pressed as disks of 8 mm diameter and 1.5 mm thick, at 15 MPa, and then, isostatically pressed at 210 MPa. The density was determined by using the Archimedes method, in as-boiled distilled water cooled to room temperature; values were corrected for temperature. The dopant concentration has been considered in the calculation of theoretical densities used to obtain relative densities.

Samples for testing in the dilatometer, Netzsch 402E, were prepared with 5 mm thickness. Heating rate was 10°C min^{-1} and the atmosphere was dry synthetic air, flowing at 30 mL min^{-1}. Considering l_o the thickness of the green compact and Δl the thickness variation ($\Delta l = l_o - l$), the linear shrinkage rate was obtained by taking the derivative of $\Delta l/l_o$ with respect to temperature. The isothermal curves were expressed in terms of a relative density normalized for green density, which is not always the same for all compacted disks. Considering d_o the density of green compacts, and that there is no weight loss during the test, the density d at a given temperature is equal to:

$$d = \frac{d_o}{(1 - \Delta l/l_o)^3} \tag{4}$$

The relative density, then, is given by $(d - d_o)/d_o$.

Twelve disks of the same composition were arranged in three piles of four disks each on alumina plates and sintered at 1300°C for 4 h, in a tubular furnace, with heating and cooling rates of 10°C min^{-1}, in a dynamic atmosphere of dry air, flowing at 150 mL min^{-1}. Only the two disks in the middle were used for characterization, except in the case of EDS (energy dispersive spectroscopy).

Microstructure analysis was carried out by measuring grain size on polished surfaces thermally etched at 1250°C for 30 min. A loss of weight was observed from those disks making contact with the alumina plates, during sintering in the tubular furnace. The resulting stains on the plates were analyzed by EDS, using a scanning electron microscope Jeol JSM T330A coupled to an X-ray analyzer series II—Noran Intruments.

3. Results and discussion

3.1. Powder characterization

Fig. 1 shows XRD patterns of the commercial SnO_2 powder and one of the Pch powders calcined at 500°C. It can be noted that both present the cassiterite phase, with a smaller degree of crystallinity for the Pch powder. No second phase is observed and, if it exists, it is beyond the apparatus detection limit. This result does not exclude the formation of a thin layer of dopant oxide on the particle surface, not detected by XRD [17, 18], which leads to the dopant segregation mentioned in the Introduction.

The particle size distribution is seen in Fig. 2. Mean particle sizes, D_{SED}, were extracted from these curves

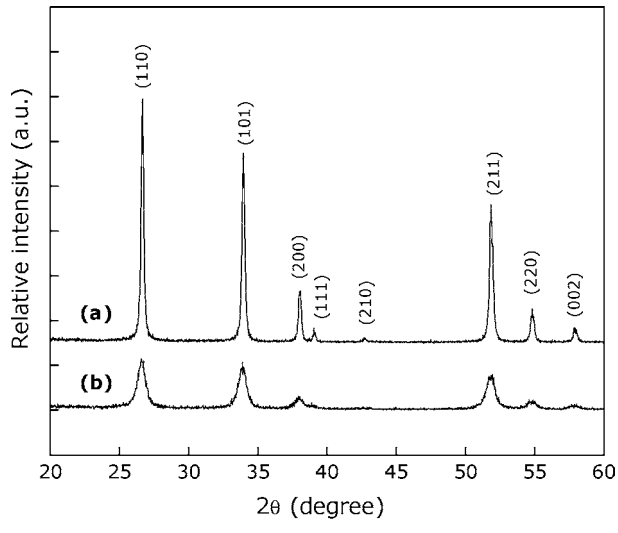

Figure 1 X-ray diffraction spectra of: (a) commercial SnO_2 and (b) $Sn_{0.98}Cu_{0.01}Sb_{0.01}$ prepared by Pch.

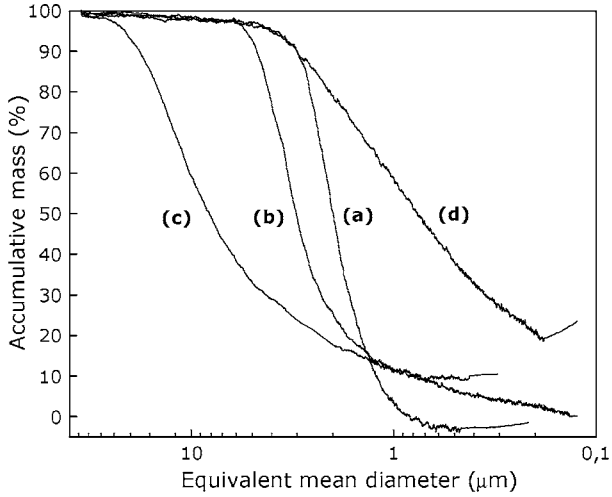

Figure 2 Particle size distributions of: (a) commercial SnO_2, (b) $Sn_{0.98}Cu_{0.01}Sb_{0.01}O_2$ (Mox), milled for 8 h, (c) $Sn_{0.98}Cu_{0.01}Sb_{0.01}O_2$ (Pch) without milling, and (d) $Sn_{0.98}Cu_{0.01}Sb_{0.01}O_2$ (Pch), milled for 8 h.

and are presented in Table I, together with values of specific surface area, S_{BET}, and mean particle size determined by BET, D_{BET}. Since S_{SED} is larger than S_{BET}, one can assume the presence of agglomerates, what was readily verified by examining the powder in a scanning electron microscope (not shown here).

It is verified that doped powders prepared by the Pch method have a surface area larger than pure SnO_2 prepared by the same method, showing that the presence of dopants affects the powder morphology, decreasing the particle size by a factor of 1.5 to 1.8. This behavior has already been observed in manganese doped SnO_2 powders prepared by the Pch method [25]. Any dopant influence is not significant in doped powders prepared by a mixture of oxides, as seen in Table I. It is also observed that doped powders prepared by the Pch method have a surface area four times larger than those prepared by a mixture of commercial oxide powders, showing that Pch powders are more reactive than commercial ones.

It is noted that milling reduces the mean agglomerate size of the Pch powder, from 7 μm to 0.75 μm, but it does not change much the particle size, around 0.029 μm. Mox powders also have agglomerates, larger than Pch ones, due to agglomerates in the commercial powder. It is also observed that the dopant oxide is always larger than the SnO_2 particle leading, probably, to local heterogeneities.

TABLE I Specific surface area and mean particle size determined by BET analysis; mean agglomerate size determined by powder sedimentation

	S_{BET} ($m^2\ g^{-1}$)		D_{BET} (μm)		D_{SED} (μm)	
System	b.m.[a]	a.m.[b]	b.m.	a.m.	b.m.	a.m.
SnO_2[c]	7.2		0.121		2	
Sb_2O_3[c]	1.9	2.8	0.572	0.380		
CuO[c]	1.4	2.0	0.664	0.464		
SnO_2[d]		20.4		0.042		
$Sn_{0.99}Cu_{0.01}O_2$[d]		32.7		0.026		
$Sn_{0.995}Cu_{0.01}Sb_{0.005}O_2$[d]		37.5		0.023		
$Sn_{0.98}Cu_{0.01}Sb_{0.01}O_2$[d]	30.2	31.2	0.029	0.028	7	0.75
$Sn_{0.99}Cu_{0.01}O_2$[e]		8.6		0.101		
$Sn_{0.995}Cu_{0.01}Sb_{0.005}O_2$[e]		9.4		0.092		
$Sn_{0.98}Cu_{0.01}Sb_{0.01}O_2$[e]		9.4		0.092		3.1

[a]b.m. and [b]a.m.—before and after milling; [c]commercial powder; [d]Pch and [e]Mox methods.

3.2. Sintering behavior

Data obtained from tests in the dilatometer are shown in Fig. 3. It can be observed that the temperature where the shrinkage rate is a maximum, i.e., maximum densification rate, is higher for the Pch method. In addition, systems prepared by Mox have, in general, maximum shrinkage rate values larger than those prepared by Pch (except for curve e). It can be noted that the width of the peaks in Fig. 3 is larger for the Pch samples. Also, it can be observed that, by increasing the antimony concentration, the temperature of maximum shrinkage rate increases and the maximum shrinkage rate decreases.

First, the results concerning the preparation method will be discussed; then, the Sb influence will be considered. In the first place, the reason for the differences in maximum shrinkage rate temperature and peak width of the shrinkage curves would be the presence of agglomerates in Pch and Mox powders, because Pch agglomerates are weaker than Mox ones. However, the state of agglomeration should not influence shrinkage at temperatures as high as 1000°C or more. Therefore, dopant segregation may have an important role in the sintering behavior of Pch and Mox compacts. Since in the Pch method the dopant cations are thought to be homogeneously distributed in the lattice, after the calcination treatment (500°C), a higher temperature is required for Cu to diffuse to the grain boundary than in the method of oxide mixture, in which Cu ions are distributed through surface diffusion at temperatures as low as 400°C [12]. Since Cu would be available on the grain surface for the sintering process at a lower temperature in the Mox system, the observed lower temperature for the maximum shrinkage rate for Mox compared with Pch ceramics is justifiable. The narrower peaks for Mox ceramics would be explained by the same reason.

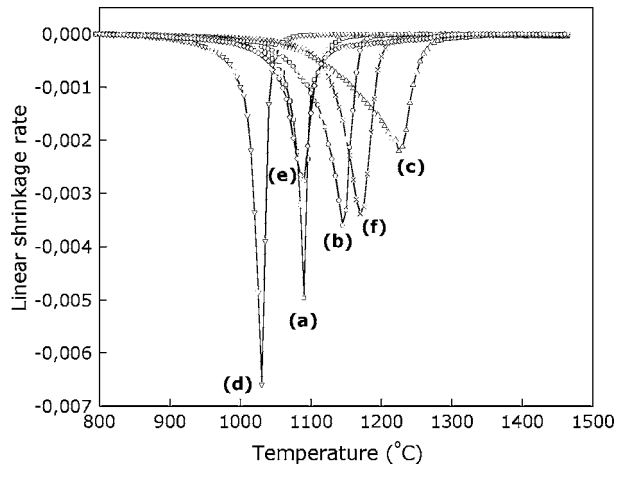

Figure 3 Linear shrinkage rate as a function of temperature of $Sn_{0.99-x}Cu_{0.01}Sb_xO_2$ systems; (a), (b), (c): Pch; (d), (e), (f): Mox; (a), (d): $x = 0$; (b), (e): $x = 0.005$; (c), (f): $x = 0.01$.

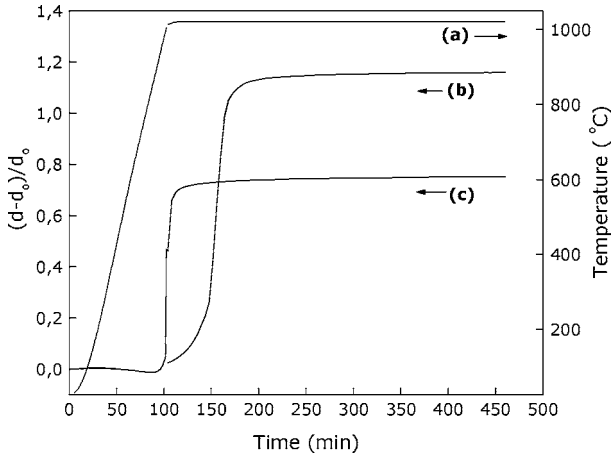

Figure 4 Isothermal shrinking curves under O_2 atmosphere at 1020°C: (a) temperature curve, (b) $Sn_{0.99}Cu_{0.01}O_2$ (Pch), and (c) $Sn_{0.99}Cu_{0.01}O_2$ (Mox).

To confirm that it is more difficult for Cu to diffuse to the grain boundary in Pch ceramics, an experiment was carried out to see if densification of Mox prepared systems started earlier than Pch ones. An isothermal experiment with the system $Sn_{0.99}Cu_{0.01}O_2$ prepared by both methods was carried out at 1020°C, the lowest temperature where both systems start to densify. The experiment was done under an oxidizing atmosphere (O_2), in order to inhibit the evaporation-condensation mechanism and the contribution of oxygen vacancy diffusion, operative at low temperatures in Cu-doped systems [12], so that the densification depended mainly on the liquid phase formation.

The two isothermal curves in Fig. 4 confirm that the densification of Mox prepared systems starts 50 min earlier than that of Pch ones, confirming that Cu diffuses more slowly to the grain boundary in Pch ceramics.

Now, the role of Sb in sintering behavior is considered. Independently of the preparation method, the effect of increasing the Sb concentration, seen in Fig. 3, was to increase the temperature of maximum shrinkage rate as well as to reduce the linear shrinkage rate. The Sb action may be associated with its reaction with oxygen vacancies [10], according to Equation 2, restraining the oxygen vacancy diffusion. By increasing the antimony concentration in both systems, the ceramics relative density decreased a little, from 98% to 95%. Although the differences observed in Fig. 3 at each addition of Sb were significant, no dramatic change occurs in the final density because of the presence of Cu and because 1% mol of Sb is not a very high concentration. This result agrees with reported data of density for SnO_2 doped with these two cations [10, 26].

Considering the results in Fig. 3, 1300°C was chosen for sintering all systems, so that they were all dense and could have their microstructures compared.

3.3. Microstructure characteristics

Microstructures of ceramics with 0.5% Sb, prepared by both methods, are shown in Fig. 5. It is observed that there are more small grains in the Pch ceramics than in the Mox ones. On the other hand, the Mox ceramics

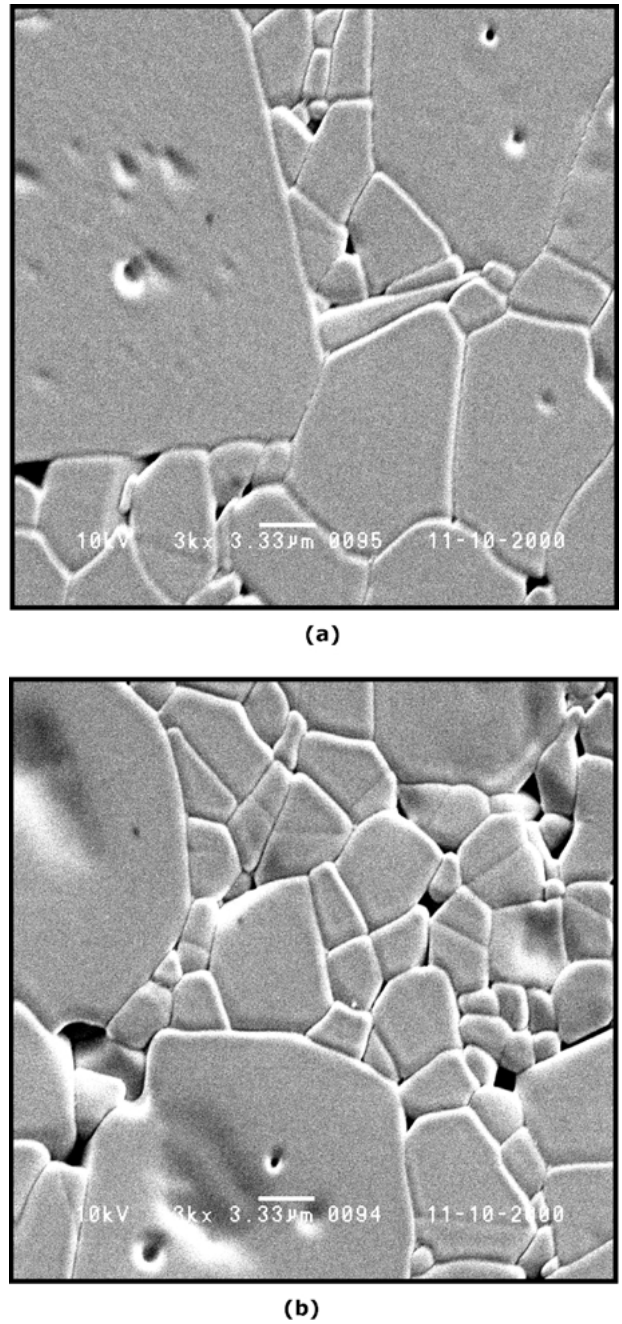

Figure 5 (a) $Sn_{0.995}Cu_{0.01}Sb_{0.005}O_2$ prepared by Mox sintered at 1300°C for 4 h and (b) $Sn_{0.995}Cu_{0.01}Sb_{0.005}O_2$ prepared by Pch sintered at 1300°C for 4 h.

have a few large grains, not present in the Pch ceramics. Also, heterogeneity in grain size distribution is clear in both ceramics. Similar behavior is found for the other two ceramics, without Sb and with 1% Sb.

In order to get a more representative result, a quantitative analysis was done, by measuring the size of at least 250 grains for both ceramics of Fig. 5. The results are shown in Fig. 6, which illustrates the cumulative number of grains as a function of grain size. For example, about 50% of all grains have sizes from 0 to 4 μm. The differences in grain size distribution observed in Fig. 5 are confirmed here.

The reason for smaller grains in the Pch ceramics is that the Pch powder has smaller particles than the Mox powder, as shown in Table I. The reason for a few larger Mox grain sizes is that coarsening acts for

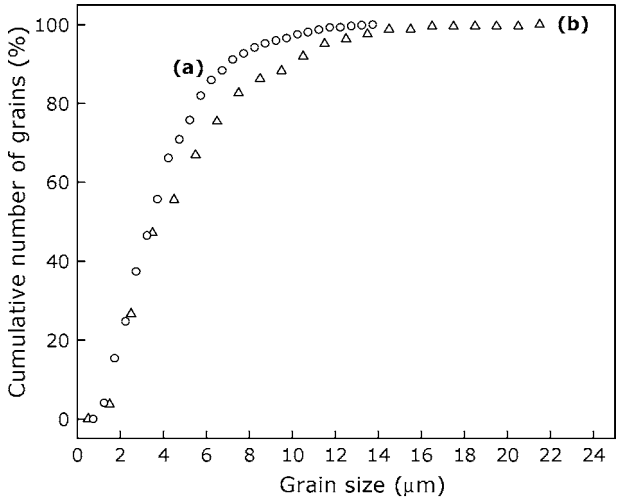

Figure 6 Cumulative number of grains in $Sn_{0.995}Cu_{0.01}Sb_{0.005}O_2$ systems as a function of grain size: (a) Pch and (b) Mox.

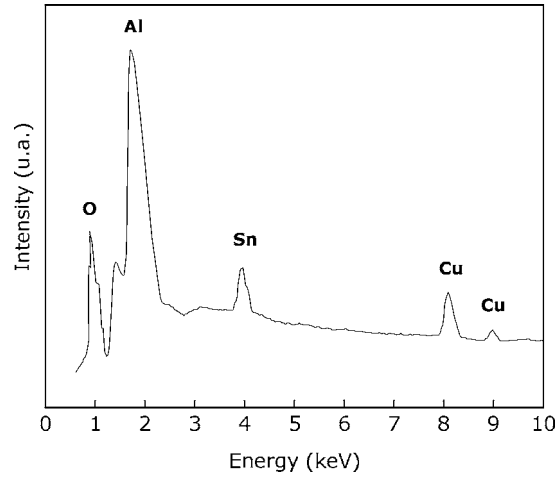

Figure 8 EDS spectrum from the stain produced by $Sn_{0.99}Cu_{0.01}$ on the alumina plate (Fig. 7).

a longer period of time in these systems, as seen in the isothermal shrinkage curves (Fig. 4). Coarsening causes the appearance of pores inside grains preferentially in Mox ceramics, because of the difference between grain growth and densification rates [27]. Coarsening is also the reason for the heterogeneity in grain size which is more evident in the Mox ceramics, since Mox powder is coaser than Pch. It was also observed, but not shown here, that the increase in the Sb concentration has a tendency of increasing grain size in both systems.

3.4. Diffusion during sintering

The stains observed on the alumina plates and corresponding EDS results are seen in Figs 7 and 8.

By weighing the discs before and after sintering, it was observed that the weight loss of Mox systems was more evident than of Pch ones. This result is in agreement with the observations of Fig. 7, because stains of Mox ceramics are somewhat darker than those of Pch ones.

In the EDS spectrum there are peaks due to Cu (K_α: 8.048 keV and 8.980 keV) and another peak between 3.5 keV and 4 keV which could be due either to Sn (L_α: 3.414 keV and 3.605 keV) or Sb (L_β: 3.929 keV and 4.132 keV). Since this line also appears in stains of ceramics without Sb, it is attributed to Sn. This spectrum is typical of all systems.

It is suggested that stains from Mox ceramics in Fig. 7 are darker than those from Pch ones because it is easier for the liquid phase containing Cu to form in the intergranular region of the Mox ceramics. More Cu would diffuse to the alumina plate, which would be responsible for the stain. This conclusion is in agreement with dilatometric results. Although SnO_2 solubility is small in the liquid phase formed by Cu [10], some of the Sn diffused to the alumina plate could be dissolved in the liquid phase.

The surfaces in contact with the alumina plates remained almost colorless for ceramics without Sb, but were dark for those with it. Thus, Cu diffuses to the plate, darkening it, while Sb remains mostly in the sample.

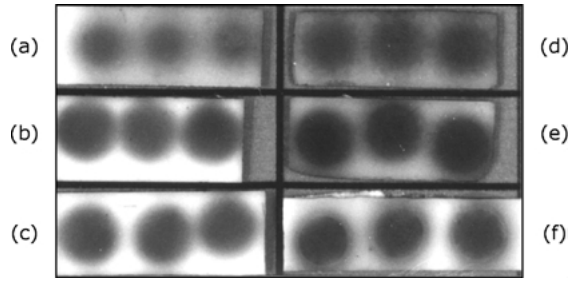

Figure 7 Stains produced by ceramics in contact with alumina plates during 1300°C sintering for 4 h: (a) $Sn_{0.99}Cu_{0.01}$Pch, (b) $Sn_{0.985}Cu_{0.01}Sb_{0.005}$Pch, (c) $Sn_{0.98}Cu_{0.01}Sb_{0.01}$Pch, (d) $Sn_{0.99}Cu_{0.01}$Mox, (e) $Sn_{0.985}Cu_{0.01}Sb_{0.005}$Mox, and (f) $Sn_{0.98}Cu_{0.01}Sb_{0.01}$Mox.

4. Conclusions

Considering that the temperature of all maximum linear shrinkage rates appeared above 1000°C, for both preparation methods, it appears that sintering involved a Cu-rich liquid phase, in a diffusion-limited process, with accentuated grain growth in the Mox ceramics. At this high temperature no intergranular phase is expected, as shown in the micrographs. However, the difference in temperature and time of maximum densification, which were larger for Pch systems, is a strong indication that Cu ions are introduced directly in to the SnO_2 lattice in the Pch system and have to diffuse to the grain surface; in the Mox ceramics Cu ions are already distributed on the particle surface, lowering the temperature for maximum shrinkage rate.

Although powder morphology, temperature of maximum densification and linear shrinkage rate were different for both preparation methods, the final relative density varied only a little because of the presence of Sb. The resultant microstructures were heterogeneous due to a coarsening process. Pch grains are smaller than Mox ones. Sn and Cu weight losses detected by EDS, were more evident for the Mox ceramics. This agrees with the sintering behavior mentioned above,

with dopant ions located in grain boundaries, from where they can diffuse to the alumina plate more easily.

Acknowledgments

The authors thank CNPq and Fapesp for financial support.

References

1. J. F. MCALEER, P. T. MOSELEY, J. O. NORRIS and D. E. WILLIAMS, *J. Chem. Soc. Faraday Trans.* **83** (1987) 1323.
2. G. TOURNIER, C. PIJOLAT, R. LALAUZEAND and B. PATISSIER, *Sens. Actuators* B **26/27** (1995) 24.
3. S. A. PIANARO, P. R. BUENO, E. LONGO and J. A. VARELA, *Ceram. Int.* **25** (1998) 1.
4. M. S. CASTRO and C. M. ALDAO, *J. Eur. Ceram. Soc.* **18** (1998) 2233.
5. D. GOUVEA, A. SMITH, J. P. BONNET and J. A. VARELA, *ibid.* **18** (1998) 345.
6. J. A. VARELA, D. GOUVÊA, E. LONGO, N. DOLET, M. ONILLON and J. P. BONNET, *Solid State Phenom.* **25/26** (1992) 259.
7. J. A. CERRI, E. R. LEITE, D. GOUVÊA, E. LONGO and J. A. VARELA, *J. Amer. Ceram. Soc.* **79** (1996) 799.
8. L. PERAZOLLI, T. R. GIRALDI, R. S. BISCARO, J. A. VARELA and E. LONGO, *Sint. Sci. and Techn.* (2000) 117.
9. N. DOLET, J. M. HEINTZ, L. RABARDEL, M. ONILLON and J. P. BONNET, *J. Mater. Sci.* **30** (1995) 365.
10. P. H. DUVIGNEAUD and D. REINHARD, *Sci. Ceram.* **12** (1980) 287.
11. J. LALANDE, R. OLLITRAULT-FICHET and P. BOCH, *J. Eur. Ceram. Soc.* **20** (2000) 2415.
12. J. P. BONNET, N. DOLET and J. M. HEINTZ, *ibid.* **16** (1996) 1163.
13. D. GOUVÊA, A. SMITH and J. P. BONNET, *Eur. J. Solid State Inorg. Chem.* **33** (1996) 1015.
14. P. A. COX, R. G. EGDELL, C. HARDING, W. R. PATTERSON and P. J. TAVENER, *Surf. Sci.* **123** (1982) 179.
15. R. G. EGDELL, W. R. FLAVELL and P. TAVENER, *J. Solid State Chem.* **51** (1984) 345.
16. W. C. LAS, N. DOLET, P. DORDOR and J. P. BONNET, *J. Appl. Phys.* **74** (1993) 6191.
17. D. SZCZUKO, J. WERNER, S. OSWALD, G. BEHR and K. WETZIG, *Appl. Surf. Sci.* **179** (2001) 301.
18. D. SZCZUKO, J. WERNER, G. BEHR, S. OSWALD and K. WETZIG, *Surf. Interface Anal.* **31** (2001) 484.
19. K. UEMATSU, N. MIZUTANI and M. KATO, *J. Mater. Sci.* **22** (1987) 915.
20. K. UEMATSU, Z. KATO, N. UCHIDA and K. SAITO, *J. Amer. Ceram. Soc.* **70** (1987) 142C.
21. M. A. ZAGHETE, J. A. VARELA, M. CILENSE, C. O. PAIVA-SANTOS, W. C. LAS and E. LONGO, *Ceram. Inter.* **25** (1999) 239.
22. D. GOUVÊA, J. A. VARELA, E. LONGO, A. SMITH and J. P. BONNET, *Eur. J. Solid State Inorg. Chem.* **30** (1993) 915.
23. I. O. MAZALI, W. C. LAS and M. CILENSE, *J. Mater. Synth. Process.* **7** (1999) 387.
24. C. V. SANTILLI and S. H. PULCINELLI, *Cerâmica* **39** (1993) 11.
25. D. GOUVEA, J. A. VARELA, A. SMITH and J. P. BONNET, *Eur. J. Solid State Inorg. Chem.* **33** (1996) 343.
26. M. R. SAHAR and M. HASBULLAH, *J. Mater. Sci.* **30** (1995) 5304.
27. Y. M. CHIANG, D. P. BIRNIE III and W. D. KINGERY, "Physical Ceramics: Principles for Ceramic Science and Engineering" (John Wiley & Sons, New York, 1997) p. 407.

Received 12 April 2002
and accepted 6 May 2003